Phonon Raman scattering in $R_{1-x}A_xMnO_{3+\delta}$ (R=La,Pr; A=Ca,Sr)

E. Granado, N. O. Moreno, A. García, J. A. Sanjurjo, C. Rettori, and I. Torriani
Instituto de Física ''Gleb Wataghin,'' UNICAMP, 13083-970, Campinas-SP, Brazil

S. B. Oseroff
San Diego State University, San Diego, California 92182

J. J. Neumeier and K. J. McClellan
Los Alamos National Laboratory, Los Alamos, New Mexico 87545

S.-W. Cheong
AT&T Bell Laboratories, Murray Hill, New Jersey 07974

Y. Tokura
Department of Physics, University of Tokyo 113, Japan
(Received 24 February 1998)

Polarized Raman spectra of single and polycrystalline $R_{1-x}A_xMnO_3$ (R=La,Pr; A=Ca,Sr) ceramic samples were studied as a function of temperature. For the rhombohedral $LaMnO_{3.1}$ and $La_{0.7}Sr_{0.3}MnO_3$, the observed Raman peaks were associated with modes arising from the folding of the Brillouin zone under lattice deformation. For the orthorhombic $LaMnO_{3.0}$, the Raman spectra are consistent with the *Pnma* structure and show an anomalous *softening* of the 494 and 604 cm^{-1} modes below the antiferromagnetic ordering temperature $T_N \simeq 140$ K. Polycrystalline samples of $La_{0.5}Ca_{0.5}MnO_3$ show a dramatic change of the Raman spectra between 100 and 160 K, which was associated with the increase of the orthorhombic distortion observed by others for $T \lesssim 240$ K. Other $R_{1-x}A_xMnO_3$ single crystals, with small orthorhombic distortions, show Raman spectra which are similar to those observed in the rhombohedral samples. [S0163-1829(98)05338-7]

I. INTRODUCTION

The concomitant metal-insulator (MI) and ferromagnetic-paramagnetic (FM-PM) transitions, induced either by temperature,[1,2] magnetic field,[2,3] or pressure,[4] in the $R_{1-x}A_xMnO_{3+\delta}$ (R=rare earth; A=alkaline earth) perovskites, have recently attracted much attention. Particularly, for $0.1 < x < 0.5$ giant negative magnetoresistance near room temperatures has been reported,[3] making these materials very attractive for future magnetic sensing applications. The $La_{1-x}Ca_xMnO_3$ compounds and some of their properties have been known since the 1950's.[1] At that time a new type of an exchange interaction, termed double exchange (DE), was proposed to explain the magnetic and transport properties of these materials. In spite of a good qualitative understanding provided by the DE model, it was recently claimed that it cannot explain quantitatively the large resistivity drop between the PM and FM phase.[5] Lattice polaron effects, enhanced by a strong Jahn-Teller coupling in Mn^{3+}, were invoked to explain the reduction in electron kinetic energy near and above the FM ordering temperature T_c. Evidences for the existence of lattice polarons has already been reported in neutron scattering[6] and isotopic T_c shift[7] experiments. Thus, the study of the phonon spectra in these compounds, by means of Raman experiments, may provide valuable information on the lattice dynamics of these materials. In this work we study (i) low-T polarized Raman spectra in single crystals of $La_{0.7}Sr_{0.3}MnO_3$ and $Pr_{0.625}Sr_{0.375}MnO_3$, (ii) low-$T$ unpolarized Raman spectra in polycrystalline $LaMnO_{3.1}$ and $La_{0.78}Ca_{0.22}MnO_3$ single crystal, and (iii) the T dependence of the Raman spectra in polycrystalline samples of $LaMnO_{3.0}$ and $La_{0.5}Ca_{0.5}MnO_3$.

II. EXPERIMENTAL DETAILS

Ceramic samples were prepared by standard ceramic methods, heating stoichiometric mixtures of the corresponding oxides as described by Oseroff *et al.*[8] The oxygen content of $LaMnO_{3+\delta}$ (or, more correctly, $La_{3/(3+\delta)}Mn_{3/(3+\delta)}O_3$, as pointed out by Ritter *et al.*[9]) samples was controlled by annealing them in oxygen and argon atmospheres. Single crystals of $La_{0.78}Ca_{0.22}MnO_3$ and $La_{0.7}Sr_{0.3}MnO_3$ were grown by the optical floating zone method. Typical rotation rates for both the seed crystal and the feed rod were 50 rpm. The crystals were grown at a rate of 6 mm/h. The $Pr_{0.625}Sr_{0.375}MnO_3$ single crystals were also grown by the floating zone method, using a lamp-image furnace.[10] The structure and phase purity were checked by x-ray powder diffraction and the crystals orientation determined by the conventional Laue method. Lattice parameters were obtained using an x-ray Rietveld refinement program.[11] The refined profiles were taken in a Rigaku R200 diffractometer and a rotating anode generator with Cu $K\alpha$ radiation. Magnetization (dc/ac) measurements were taken in Quantum Design PPMS and MPMS-SQUID magnetometers. Electron spin resonance (ESR) experiments were carried out in a Varian X-band spectrometer using a room-T rectangular TE_{102} cavity and a He gas flux T controller. The Raman

TABLE I. Structures and lattice parameters of the studied compounds at room temperature.

Sample	Space group	**a** (Å)	$\mathbf{b}/\sqrt{2}$ (Å)	**c** (Å)	$\alpha(°)$
$La_{0.7}Sr_{0.3}MnO_3$	D_{3d}^6	5.434(1)			60.437
$LaMnO_{3.1}$	D_{3d}^6	5.475(1)			60.583
$LaMnO_{3.0}$	D_{2h}^{16}	5.724(1)	5.442(1)	5.534(1)	
$La_{0.78}Ca_{0.22}MnO_3$	D_{2h}^{16}	5.501(1)	5.481(1)	5.479(1)	
$La_{0.5}Ca_{0.5}MnO_3$	D_{2h}^{16}	5.427(1)	5.402(1)	5.418(1)	
$Pr_{0.625}Sr_{0.375}MnO_3$	D_{2h}^{16}	5.486(1)	5.438(1)	5.447(1)	

measurements were performed in a backscattering geometry using a Jobin Yvon T64000 triple spectrometer equipped with a cryogenic charge-coupled device camera, using the 514.5 nm line of an argon ion laser. The absolute Raman shifts are measured within a precision of $2\ \mathrm{cm}^{-1}$. The samples were mounted on the cold finger end of a closed-cycle He refrigerator. The sample T was measured, within an accuracy of 2 K, using a gold-chromel thermocouple mounted on the same cold finger end. In order to avoid heating of the sample, the incident laser power was kept below 15 mW focused in a diameter of $\sim 50\ \mu$m. To minimize surface decomposition effects, all the spectra were taken on fresh broken surfaces, exposed to the air for a few minutes before being measured. All the Raman measurements as a function of T were done increasing the temperature.

III. NORMAL MODE ANALYSIS

The ideal perovskite ABO_3 of cubic structure (space group O_h^1, $Pm3m$) presents 15 normal modes of vibration. These modes correspond to the following irreducible representations at the zone center:

$$\Gamma(O_h^1) = 4F_{1u} + F_{2u}, \tag{1}$$

where one of the F_{1u} irreducible representations corresponds to a triple degenerate acoustical mode. The other three F_{1u} irreducible representations are the infrared (IR) active optical modes, allowed for cubic symmetry. The lowest frequency (external mode) corresponds to a vibration of the A ions against the rigid BO_6 octahedra. The intermediate frequency (bending mode), corresponds to a vibration where the B ion and two apical oxygens move against the other four oxygens of the octahedron. At the highest frequency (stretching mode), the B ion moves against the rigid oxygen octahedron. Finally, the F_{2u} irreducible representation corresponds to a silent mode, which is not IR nor Raman active.[12,13] Recent IR reflectivity experiments in $La_{0.7}Ca_{0.3}MnO_3$ showed three IR active modes at about 170, 330, and 580 cm^{-1}.[14] At a perfect perovskite of cubic structure all lattice sites have inversion symmetry. Therefore, first order Raman scattering is forbidden.

Samples of $LaMnO_{3+\delta}$ treated in oxygen present rhombohedral crystal structure, space group D_{3d}^6 ($R_{\bar{3}C}$), with two formulas per unit cell.[15] In the ABO_3 perovskites this space group is generated by the rotation of the BO_6 octahedra about the cubic [111] directions. These rotations occur in opposite directions in adjacent unit cells. Thus, the 30 vibrational degrees of freedom per unit cell result in the following modes at the zone center:

$$\Gamma(D_{3d}^6) = 2A_{1u} + 3A_{2g} + A_{1g} + 4A_{2u} + 4E_g + 6E_u, \tag{2}$$

where the A_{1g} and the four E_g modes are Raman active. The Raman active modes are associated to R(1/2,1/2,1/2)-point Brillouin zone boundary modes in the cubic phase, which become zone center modes because the Brillouin zone is halved in the rhombohedral phase.[16,17] A series of isostructural rare earth aluminate crystals ($LaAlO_3$, $PrAlO_3$, $NdAlO_3$, etc.) show a $D_{3d} \rightarrow O_h$ phase transition as a function of T driven by the softening of the $\Gamma_{25}(F_{2u})$-mode branch at the R(1/2,1/2,1/2) point of the high-T Brillouin zone.[18,19]

$LaMnO_{3.0}$ shows O' orthorhombic ($\mathbf{b}/\sqrt{2} < \mathbf{c} < \mathbf{a}$) structure, space group D_{2h}^{16} ($Pnma$).[20] In this structure, the MnO_6 octahedra have different Mn-O bond lengths and are rotated around the cubic [010] and [101] axes. It is normally accepted that a cooperative static Jahn-Teller effect at the Mn^{3+} site is responsible for this distorted perovskite.[21] Room-temperature Raman measurements in $LaMnO_{3.0}$ have been recently reported and analyzed by Iliev *et al.*[22] The primitive unit cell has four formula units giving 60 Γ-point vibrational modes. Factor group analysis yields the following symmetry distribution of these modes at the zone center:

$$\Gamma(D_{2h}^{16}) = 8A_u + 10B_{1u} + 8B_{2u} + 10B_{3u} + 7A_g + 5B_{1g} + 7B_{2g} + 5B_{3g}, \tag{3}$$

where the $7A_g + 5B_{1g} + 7B_{2g} + 5B_{3g}$ modes are Raman active. In the orthorhombic phase not only the modes arising from the R(1/2,1/2,1/2) point of the Brillouin zone of cubic phase become zone center, but also those arising from the (1/2,0,1/2) and the (0,1/2,0) points.

The perovskites $R_{1-x}A_xMnO_{3+\delta}$ (R = rare earth; A = alkaline earth) show decreasing deviations from the ideal cubic structure upon doping.[23] This is attributed to a reduction in the static Jahn-Teller distortion due to the presence of Mn^{4+}.[24] The structures of the (LaCa)MnO_3 and (PrSr)MnO_3 systems are generally refined with an orthorhombic D_{2h}^{16} space group for all concentrations.[25,26] The (LaSr)MnO_3 system has D_{2h}^{16} symmetry for $x < 0.17$ and rhombohedral symmetry D_{3d}^6 for $x > 0.17$. In addition, it presents a structural phase transition induced either by T or H for $x \approx 0.17$.[27]

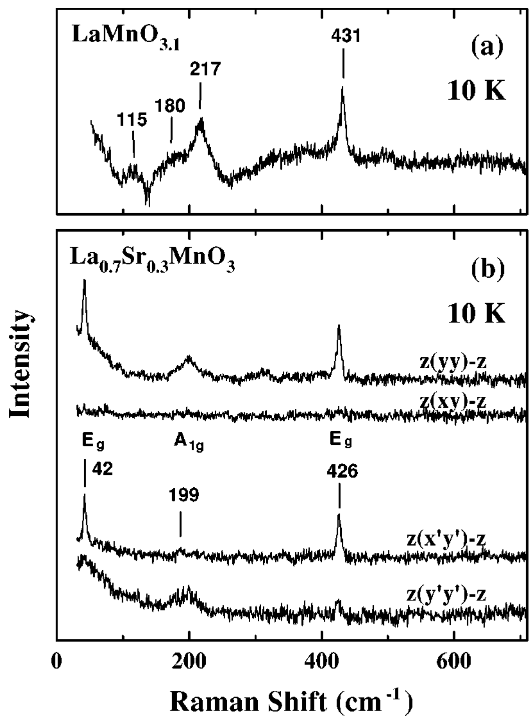

FIG. 1. Raman spectra, at $T=10$ K, of the rhombohedral samples: (a) $\mathrm{LaMnO}_{3.1}$ oxygen annealed polycrystalline ceramic sample and (b) $\mathrm{La}_{0.7}\mathrm{Sr}_{0.3}\mathrm{MnO}_3$ single crystal for different polarizations. The x, y, and z directions correspond to cubic [100] axes (Mn-O-Mn), and x' and y' indicate the cubic [110] directions (La-O-La).

IV. RESULTS AND DISCUSSION

Table I gives the crystal structure and room temperature lattice parameters for all the studied samples. Figures 1(a) and 1(b) show, respectively, the Raman spectra at $T=10$ K of an oxygen annealed polycrystalline ceramic sample of $\mathrm{LaMnO}_{3.1}$ and of a single crystal of $\mathrm{La}_{0.7}\mathrm{Sr}_{0.3}\mathrm{MnO}_3$ at different polarizations. The x, y, and z directions correspond to the [100] cubic axes (Mn-O-Mn directions), and x' and y' indicate the cubic [110] directions. Both samples are rhombohedral D_{3d}^6 space group. The main features of the Raman spectra for both samples are similar. For $\mathrm{La}_{0.7}\mathrm{Sr}_{0.3}\mathrm{MnO}_3$ the peak at 199 cm^{-1} is much stronger in parallel polarization, thus, it is an A_{1g} mode. The peaks at 42 and 426 cm^{-1} are observed in crossed $z(x'y')$-z polarization, thus, they have E_g symmetry. Table II gives, for our samples and some isomorphous rare-earth aluminates,[18,19] the correlation between the observed D_{3d}^6 zone-center Raman active phonons and the $R(1/2,1/2,1/2)$-point phonons of the O_h^1 perovskite structure. The shoulder at $\sim$180 cm^{-1} in $\mathrm{LaMnO}_{3.1}$ may be associated to a splitting of the 217 cm^{-1} A_{1g} mode, induced by defects of the crystal lattice. Such defects must be present in this sample as a consequence of the excess of oxygen. We should mention that the A_{1g} mode is much broader than the E_g modes also for the $\mathrm{La}_{0.7}\mathrm{Sr}_{0.3}\mathrm{MnO}_3$ single crystal, and is probably very sensitive to defects of the crystal lattice. For $\mathrm{La}_{0.7}\mathrm{Sr}_{0.3}\mathrm{MnO}_3$, spectra taken on a surface exposed to the air during few weeks present also two broad peaks at $\sim$490 and $\sim$640 cm^{-1} (not shown), which disappear in measurements taken on fresh surfaces. Notice that the frequencies of these modes are near the intense 494 and 604 cm^{-1} modes of the orthorhombic phase of LaMnO_3 (see below). Therefore, we attribute these peaks to scattering induced by orthorhombically distorted regions which may be present in old surfaces. This kind of surface degradation was observed in almost all our samples. Recently, Iliev *et al.*[22] reported a room-temperature Raman spectrum of a rhombohedral sample of LaMnO_3 showing broad peaks at 220, $\sim$490, and $\sim$610 cm^{-1}. The last two peaks are not observed in the present work for fresh surfaces of rhombohedral samples, and we believe they are also due to orthorhombic distortions which may be present on their sample.

Figure 2 shows the Raman spectra at 15 K of an argon annealed polycrystalline ceramic sample of $\mathrm{LaMnO}_{3.0}$. This sample is orthorhombic D_{2h}^{16} space group ($Pnma$), with a large deviation from the cubic perovskite structure. The Raman spectrum shows 14 peaks at 94, 110, 143, 192, 205, 261, 290, 308, 326, 433, 448, 494, 604, and 643 cm^{-1}. Except for the 94 cm^{-1} peak, the spectrum of Fig. 2 is consistent with much less resolved spectra at $T=300$ K and lattice dynamic calculations reported by Iliev *et al.*[22] Then, the 94 cm^{-1} peak may be associated to a small amount of a

TABLE II. Correlation for the Raman active phonons at the point Γ in the D_{3d}^6 Brillouin zone and at point R in the O_h^1 Brilloiun zone. A tentative assignment of the Raman phonon frequencies at 10 K in $\mathrm{La}_{0.7}\mathrm{Sr}_{0.3}\mathrm{MnO}_3$ and $\mathrm{LaMnO}_{3.1}$, together with published data in other rhombohedral ABO_3 perovskites are also shown.

Approximate eigenvector	O_h^1 mode symmetry	D_{3d}^6 mode symmetry	Phonon frequencies (cm^{-1}) $\mathrm{La}_{0.7}\mathrm{Sr}_{0.3}\mathrm{MnO}_3$ 10 K	$\mathrm{LaMnO}_{3.1}$ 10 K	PrAlO_3 [a] 212 K	NdAlO3 [a] 300 K
Rotation of oxygen cage	$F_{2u}(R)(\Gamma_{25})$	$E_g(\Gamma)$	42		45	50
		$A_{1g}(\Gamma)$	199	217	222	241
Motion of A ion	$F_{1u}(R)$ (Γ_{15})	$E_g(\Gamma)$		115	164	
Internal vibration of oxygen cage	$E_u(R)$ (Γ'_{12})	$E_g(\Gamma)$				
	$F_{1u}(R)$ (Γ_{15})	$E_g(\Gamma)$	426	431	506	509

[a]See Refs. 18 and 19.

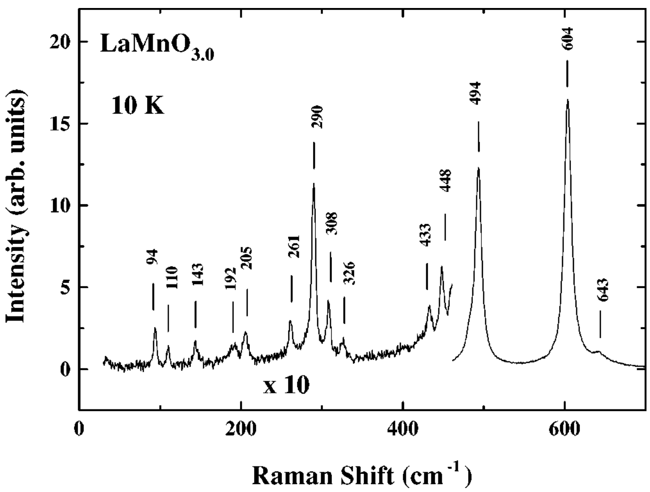

FIG. 2. Raman spectrum, at $T=10$ K, of the orthorhombic $LaMnO_{3.0}$ argon annealed polycrystalline ceramic sample.

spurious phase in our sample, not detected by our x-ray measurements.

Figures 3(a) and 3(b) show, respectively, for the three most intense Raman peaks of Fig. 2 (290, 494, and 604 cm^{-1}), the T dependence of their frequency and linewidth, obtained from the best fit to Lorentzian line shapes. Notice that the 494 and 604 cm^{-1} peaks present an anomalous softening of the frequency for $T \lesssim 150$ K. No anomaly was observed in the T dependence of the linewidth for these peaks. Recent lattice dynamic calculations for orthorhombic $LaMnO_3$ (Ref. 22) indicate that the 604 cm^{-1} peak corresponds to an in-phase stretching mode of the oxygen cage. In this mode, the O^{2-} ions of the xz plane vibrate in the Mn-O direction. The same calculations indicate that the 494 cm^{-1} peak is associated to an out-of-phase bending mode of the oxygen cage, where the O^{2-} ions vibrate perpendicularly to the Mn-O line. Finally, the 290 cm^{-1} peak is attributed to an out-of-phase x rotation of the oxygen cage, and therefore does not involve internal distortions of the MnO_6 octahedra.[22]

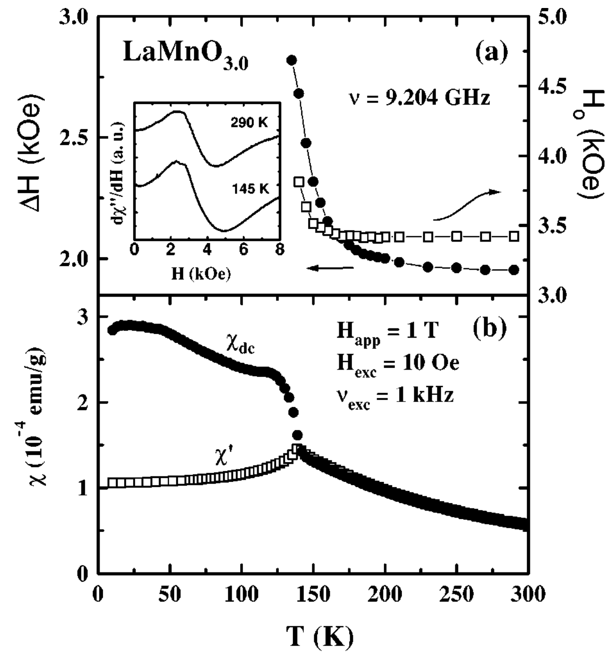

FIG. 4. T dependence of the (a) ESR linewidth and resonance field for the sample of Fig. 2 and (b) dc (χ_{dc}) and ac (χ') susceptibilities for the same sample, measured under an applied field of 1 T. χ' is frequency independent between 1 and 10 kHz.

Figures 4(a) and 4(b) show, respectively, the ESR and dc/ac-susceptibility data for the $LaMnO_{3.0}$ sample of Fig. 2. In agreement with earlier neutron scattering[28] and recent magnetization[9] experiments, the data in Fig. 4 show that our $LaMnO_{3.0}$ sample experience an antiferromagnetic (AFM) and weak ferromagnetic (WFM) ordering at $T \simeq 140$ K. In the paramagnetic region, 140 K$\lesssim T \lesssim$300 K, a Curie-Weiss $[\chi^{-1}=(T+\theta)/C]$ fitting of the susceptibility data yields $\theta=-40(5)$ K and $\mu_{eff}=5.4(4)\mu_B$. The number of Bohr magnetons is consistent with that expected for Mn^{3+}, $\mu_{eff} \approx 4.9\mu_B$ $(g=2, S=2)$. In addition, the intensity of the ESR line, when compared with calibrated standards, indicates that the resonance is also associated to Mn^{3+}.

It is known that in some AFM and FM transition metal oxides compounds, optical modes present frequency anomalies below the ordering temperature. In the AFM isostructural $YCrO_3$ the 568 cm^{-1} B_{2g} mode, corresponding to our 604 cm^{-1} mode in $LaMnO_{3.0}$, shows an anomalous hardening of ~ 10 cm^{-1} which was correlated to the lattice unit cell volume contraction observed below T_N.[29] In the FM $La_{0.7}Ca_{0.3}MnO_3$, IR reflectivity measurements showed ~ 15 cm^{-1} hardening of the 580 cm^{-1} stretching mode at $T \lesssim T_c$.[14] Also in this case the anomaly was correlated to the anomalous change of ~ 0.001Å found in the quasicubic **a** parameter (average Mn-Mn distance) near T_c. It is evident from these results that frequency anomalies of some optical modes may be expected as a consequence of magnetostrictive effects. Therefore, the anomalous softening shown in

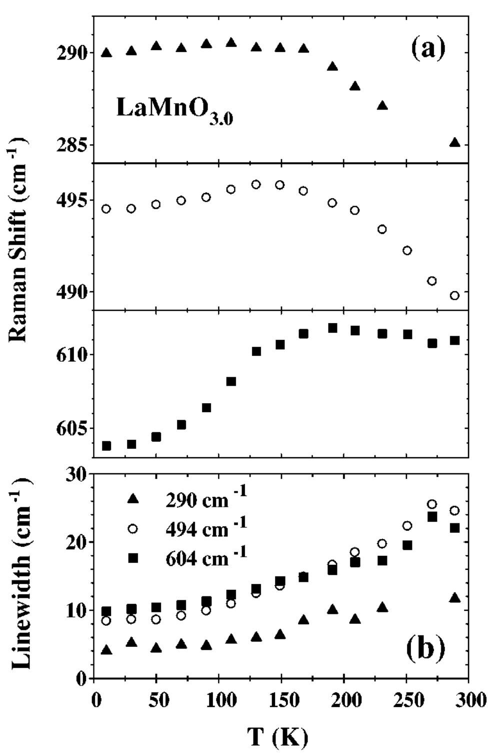

FIG. 3. T dependence of the (a) Raman shift and (b) linewidth for the 290, 494, and 604 cm^{-1} peaks of Fig. 2.

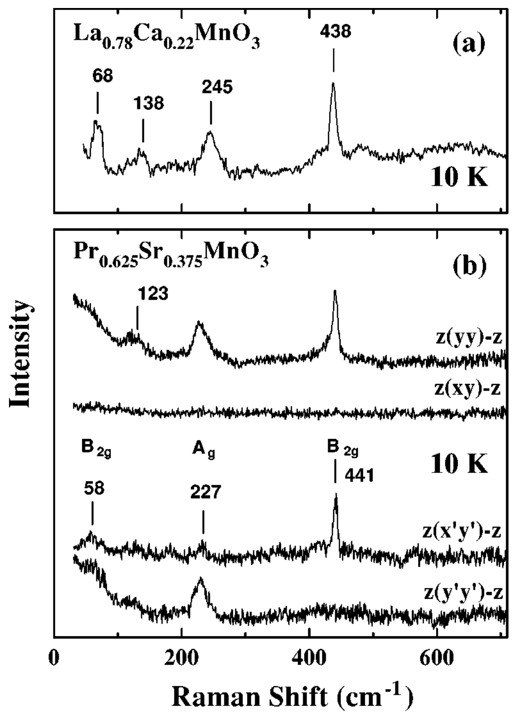

FIG. 5. Raman spectra, at $T=10$ K, of the orthorhombic single crystals (a) $La_{0.78}Ca_{0.22}MnO_3$ unpolarized and (b) $Pr_{0.625}Sr_{0.375}MnO_3$ polarized. The x, y, z, x', and y' directions are the same as those of Fig. 1.

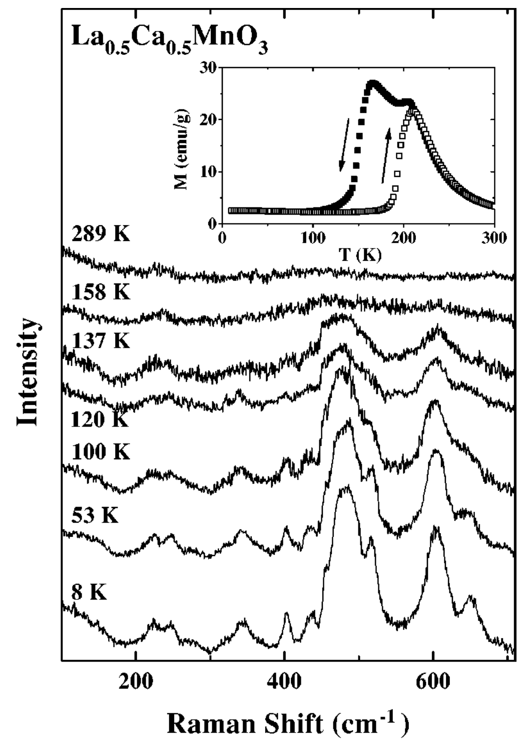

FIG. 6. T dependence of the Raman spectra for the $La_{0.5}Ca_{0.5}MnO_3$ polycrystalline ceramic sample. Inset: T dependence of the dc-susceptibility for the same sample at $H_{app}=1$ T, measured on cooling (filled) and warming (open).

Fig. 3(a) for the 494 and 604 cm^{-1} modes in $LaMnO_{3.0}$ may also be caused by a change in the lattice parameters at $T_N \lesssim 150$ K. Recent neutron diffraction experiments in stoichiometric $LaMnO_3$ measured the T dependence of the lattice parameters.[9] The small anomalies observed in the **a** and **c** ($Pnma$) lattice parameters at $T\approx 140$ K may be the origin for the anomalous softening of the 494 and 604 cm^{-1} modes. Notice that, as mentioned above, very small lattice parameter deviation from the normal Gruneisen law may produce a relatively large anomaly in some of the optical modes.[14] Nevertheless, to the best of our knowledge, this is the first report on a softening of optical modes associated with magnetic ordering.

Figures 5(a) and 5(b) show, respectively, the unpolarized and polarized Raman spectra at 10 K for the $La_{0.78}Ca_{0.22}MnO_3$ and $Pr_{0.625}Sr_{0.375}MnO_3$ single crystals. The lattice parameters given in Table I indicate that the orthorhombic distortion in these samples are much smaller than that in $LaMnO_{3.0}$. The Raman spectra shown in Fig. 5 are very similar for both crystals. The main peaks are at 58, 123, 227, and 441 cm^{-1} for $Pr_{0.625}Sr_{0.375}MnO_3$ and at 68, 138, 245, and 438 cm^{-1} for $La_{0.78}Ca_{0.22}MnO_3$. Comparing these spectra to those of Fig. 1, one observes that rhombohedral manganites and slightly orthorhombic distorted manganites have similar Raman spectra. These results suggest that for a small orthorhombic distortion, the main Raman features may be originated at the R-point Brillouin zone boundary phonons in the cubic phase, as in the case of the rhombohedral D_{3d}^6 perovskites. Due to the small orthorhombic distortion and/or twinning effects, it was not possible to determine the direction of the long axis (**b**) of the orthorhombic unit cell for the $Pr_{0.625}Sr_{0.375}MnO_3$ single crystal. The 227 cm^{-1} peak appears in parallel polarization, therefore it is an A_g mode. Simple calculations show that for $z(x'y')$-z polarization the B_{1g} and B_{3g} modes are forbidden for any orientation of the long axis along the Mn-O-Mn directions. Therefore, the 58 and 441 cm^{-1} modes, observed in this polarization, should correspond to a B_{2g} mode.

Figure 6 shows that for the polycrystalline sample of $La_{0.5}Ca_{0.5}MnO_3$ the Raman spectra change dramatically between 100 and 160 K. Notice that the strong structures at $\sim$500 and $\sim$600 cm^{-1} disappear at high T. The comparison with Fig. 2 suggests that these peaks may be associated to the strong 494 and 604 cm^{-1} modes in the orthorhombic $LaMnO_{3.0}$. These results suggest that the $La_{0.5}Ca_{0.5}MnO_3$ sample becomes strong orthorhombically distorted at low T. The disappearance of these peaks at high T indicates that the sample structure become nearly cubic. The dc magnetization for the same sample is shown in the inset of Fig. 6, measured on field cooling (FC) and warming after field cooling (FCW), with an applied field (H_{app}) of 1 T. The data shows FM-AFM transitions occurring at 135 K$\lesssim T_{Mag}^{FC} \lesssim 165$ K and 185 K$\lesssim T_{Mag}^{FCW} \lesssim 210$ K. Similar measurements taken with $H_{app}=100$ Oe present the same transition temperatures. These results are in general agreement with high resolution synchrotron x-ray and neutron powder diffraction studies on the same compound, where large lattice parameters change at the FM-AFM transitions were observed.[25,30] However, it is a large difference in the transition temperatures obtained by Raman scattering ($100\,\mathrm{K} \lesssim T_{Raman}^{fresh} \lesssim 160$ K) and dc-magnetization experiments (185 K$\lesssim T_{Mag}^{FCW} \lesssim 210$ K) is seen; both measured increasing T. In contrast, the temperature range where large lattice parameter changes were observed, measured on warming (180 K$\lesssim T_{\rm Lattice}^{\rm Warm}\lesssim$240 K),[30] is very close to $T_{\rm Mag}^{\rm FCW}$. For the Raman measurements in this sample, the incident laser power was particularly low ($\sim$5 mW), therefore laser heating can hardly account for this large T difference. We suggest that due to the delicate stoichiometry dependence of this compound, the surface properties may present slight differences from those of the bulk, even for surfaces exposed to the air during few minutes. In order to check this point, we performed the same measurements on an old surface of the same sample, and the Raman transition was shifted to even lower temperatures (50 K$\lesssim T_{\rm Raman}^{\rm old}\lesssim$100 K). Nevertheless, a more detailed study is still needed to clarify this point.

V. CONCLUSIONS

In summary, we have studied the Raman spectra of the $R_{1-x}A_x$MnO$_{3+\delta}$ (R=La,Pr; A=Ca,Sr) manganites with different degrees of deviations from the ideal cubic perovskite structure. For rhombohedral and slightly distorted orthorhombic samples, the main modes were assigned to R-point modes of the cubic structure, which become Raman active due to the folding of the Brillouin zone. For strongly distorted orthorhombic samples a wide variety of modes appear, but less than the 24 modes allowed for this symmetry. For the argon annealed $LaMnO_{3.0}$ sample the 494 and 604 cm^{-1} modes present an anomalous softening for $T\lesssim$150 K of $\sim$1 and $\sim$8 cm^{-1}, respectively. These softenings were associated to the AFM ordering experienced by this sample and observed by ESR and dc/ac susceptibility measurements. The $La_{0.5}Ca_{0.5}MnO_3$ sample shows a dramatic change of the Raman spectra between 100 and 160 K, which we attributed to the large orthorhombic distortion reported by others in this compound at low T.

ACKNOWLEDGMENTS

This work was supported by FAPESP Grant No 95/4721-4, São Paulo-SP-Brazil, NSF-DMR Grant No. 9705155, and NSF-INT Grant No. 9602928.

[1] G.M. Jonker and J.H. van Santen, Physica (Utrecht) **16**, 337 (1950).
[2] K.M. Kusters, J. Singleton, D.A. Keen, R. McGreevy, and W. Hayes, Physica B **155**, 362 (1989).
[3] R. von Helmolt, J. Wecker, B. Holzapfel, L. Schultz, and K. Samwer, Phys. Rev. Lett. **71**, 2331 (1993).
[4] H.Y. Hwang, T.T.M. Palstra, S.-W. Cheong, and B. Batlogg, Phys. Rev. B **52**, 15 046 (1995).
[5] A.J. Millis, P.B. Littlewood, and B.I. Shraiman, Phys. Rev. Lett. **74**, 5144 (1995); A.J. Millis, Phys. Rev. B **53**, 8434 (1996); A.J. Millis, B.I. Shraiman, and R. Mueller, Phys. Rev. Lett. **77**, 175 (1996).
[6] S.J.L. Billinge, R.G. DiFrancesco, G.H. Kwei, J.J. Neumeier, and J.D. Thompson, Phys. Rev. Lett. **77**, 715 (1996); P. Dai, J. Zhang, H.A. Mook, S.-H. Liou, P.A. Dowben, and E.W. Plummer, Phys. Rev. B **54**, R3694 (1996).
[7] G. Zhao, K. Conder, H. Keller, and K.A. Muller, Nature (London) **381**, 676 (1996).
[8] S.B. Oseroff, M. Torikachvili, J. Singley, S. Ali, S.-W. Cheong, and S. Schultz, Phys. Rev. B **53**, 6521 (1996).
[9] C. Ritter, M.R. Ibarra, J.M. De Teresa, P.A. Algarabel, C. Marquina, J. Blasco, J. García, S. Oseroff, and S-W. Cheong, Phys. Rev. B **56**, 8902 (1997).
[10] A. Urushibara, Y. Moritomo, T. Arima, A. Asamitsu, G. Kido, and Y. Tokura, Phys. Rev. B **51**, 14 103 (1995).
[11] D.B. Wiles and R.A. Young, J. Appl. Crystallogr. **14**, 149 (1981).
[12] J.T. Last, Phys. Rev. **105**, 1740 (1957).
[13] B.D. Silverman and G.F. Koster, Z. Phys. **163**, 158 (1961).
[14] K.H. Kim, J.Y. Gu, H.S. Choi, G.W. Park, and T.W. Noh, Phys. Rev. Lett. **77**, 1877 (1996).
[15] M. Verelst, N. Rangavittal, C.N.R. Rao, and A. Rousset, J. Solid State Chem. **104**, 74 (1993).
[16] W. Cochran and A. Zia, Phys. Status Solidi **25**, 273 (1968).
[17] H. Thomas and K.A. Muller, Phys. Rev. Lett. **21**, 1256 (1968).
[18] J.F. Scott, Phys. Rev. **183**, 823 (1969).
[19] R.T. Harley, W. Hayes, A.M. Perry, and S.R.P. Smith, J. Phys. C **6**, 2382 (1973).
[20] J.B. Goodenough and J.M. Longo, in *Magnetic and Other Properties of Oxides and Related Compounds*, edited by K.-H. Hellwege and A. M. Hellwege, Landolt-Borstein, Tabellen, New Series, Group 3, Vol. 4, Pt. a (Springer-Verlag, Berlin, 1970), p. 126.
[21] A.A. Elemans, B. van Laab, K.R. Van der Veen, and B.O. Loopstra, J. Solid State Chem. **3**, 238 (1971).
[22] M.N. Iliev, M.V. Abrashev, H.-G. Lee, V.N. Popov, Y.Y. Sun, C. Thomsen, R.L. Meng, and C.W. Chu, Phys. Rev. B **57**, 2872 (1998).
[23] A. Wold and R. Arnott, J. Phys. Chem. Solids **9**, 176 (1959).
[24] J.B. Goodenough, A. Wold, R.J. Arnott, and N. Menyuk, Phys. Rev. **124**, 373 (1961).
[25] P.G. Radaelli, D.E. Cox, M. Marezio, S.-W. Cheong, P.E. Schiffer, and A.P. Ramirez, Phys. Rev. Lett. **75**, 4488 (1995).
[26] K. Knízek, Z. Jirák, E. Pollert, F. Zounová, and S. Vratislav, J. Solid State Chem. **100**, 292 (1992).
[27] A. Asamitsu, Y. Moritomo, Y. Tomioka, T. Arima, and Y. Tokura, Nature (London) **373**, 407 (1995); J. Mitchell, D.N. Argyriou, C.D. Potter, D.G Hinks, J.D. Jorgensen, and S.D. Bader, Phys. Rev. **54**, 6172 (1996).
[28] E.O. Wollan and W.C. Koehler, Phys. Rev. **100**, 545 (1955).
[29] M. Udagawa, K. Kohn, N. Kashizuka, and T. Tsushima, Solid State Commun. **16**, 779 (1975).
[30] P.G. Radaelli, D.E. Cox, M. Marezio, and S.-W. Cheong, Phys. Rev. B **55**, 3015 (1997).